Materials Research Express

PAPER

Modelling and optimizing surface roughness and MRR in electropolishing of AISI 4340 low alloy steel in eco-friendly NaCl based electrolyte using RSM

Mohammad Meghdad Fallah[1], **Milad Aghaee Attar**[2], **Amir Mohammadpour**[1], **Mahmoud Moradi**[3] and **Noureddine Barka**[4]

[1] Department of Mechanical Engineering, Shahid Rajaee Teacher Training University, Tehran, Iran
[2] Department of Mechanical Engineering, Faculty of Engineering, K.N. Toosi University of Technology, Tehran, Iran
[3] School of Mechanical, Aerospace and Automotive Engineering, Faculty of Engineering, Environment and Computing, Coventry University, Gulson Road, Coventry, CV1 2JH, United Kingdom
[4] Department of Mathematics, Computer Science and Engineering, Université du Québec à Rimouski, Rimouski, Québec, Canada

E-mail: m.fallah@sru.ac.ir

Keywords: electropolishing (EP), response surface method (RSM), AISI 4340 low alloy steel, COMSOL multiphysics, Derringer's desirability approach

OPEN ACCESS

RECEIVED
15 April 2021

REVISED
1 October 2021

ACCEPTED FOR PUBLICATION
20 October 2021

PUBLISHED
29 October 2021

Abstract

Electropolishing (EP) is a reliable post-processing method of the drilled metals for achieving a high-quality surface finish with an appropriate material removal rate. This process has many applications due to its advantages such as improving the surface quality by removing the surface peaks on a micro-scale. The aim of most attempts on this process is setting up the optimum parameters to obtain maximum Material Removal Rate (MRR) with minimum surface roughness. In the present wo k, electropolishing of AISI 4340 low alloy steel immersed in eco-friendly NaCl solution has been studied numerically and experimentally. So, primarily a simulation model was developed for the EP process on cylinder parts in COMSOL Multiphysics which was validated with experimental approaches. The results revealed that the numerical model would be convenient for EP. The experiments were performed using Response Surface Methodology (RSM) to evaluate the effect of input variables on the responses. The effects of input variables electrolyte temperature, current intensity, and primary gap were investigated on the outputs MRR and surface roughness at five levels. Based on the results, the electrolyte temperature and current intensity were more effective parameters on the outputs. Results of ANOVA and regression analysis approach revealed that by increasing the current and electrolyte temperature, the MRR increases correspondingly and surface roughness declines and the primary gap has a reverse effect on the MRR. Finally, by performing a multi-objective optimization using Derringer's desirability approach, the EP of AISI 4340 with an eco-friendly NaCl solution was optimized.

1. Introduction

In electrochemical machining, a shaped tool as cathode penetrates into the workpiece (the anode) continuously and by passing the high-velocity electrolyte through their gap, an atom by atom material removal performs [1]. Electropolishing (EP) which is known as electrochemical polishing, anodic polishing, or electrolytic polishing is an electrochemical process in which anodic dissolution between cathode and anode occurs in a specific electrolyte solution. The difference is that electrochemical machining is a shaping process while electropolishing is a finishing process. A schematic setup of the electropolishing process is shown in figure 1.

EP is used to improve the surface quality of metallic parts as well as to passivate the surfaces. Since the electropolishing is a non-contact process, the polish marks and deformed layers do not remain on the part surface and so the durability of EP processed part will be longer than traditionally polished parts. Comparing

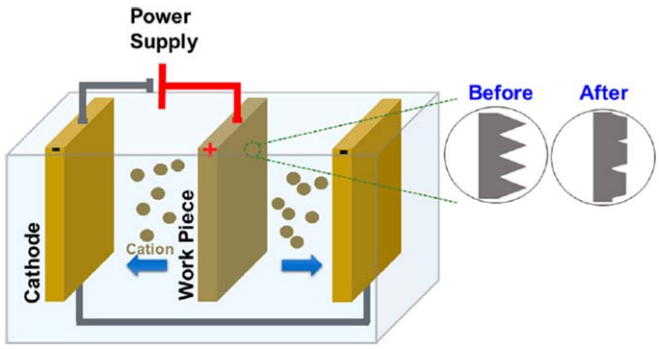

Figure 1. Schematic illustration of a typical setup of the electrolytic cell for electropolishing [2] 2017, reprinted by permission of the publisher (Taylor & Francis Ltd, http://www.tandfonline.com.)

with the other common mechanical polishing methods, EP is a damage-free process without any residual stress, as well, it can be said that the electropolishing process enhances the corrosion resistance of metals, which is especially vital for advanced applications. Corrosion resistance extensively depends on the texture property of the surface, so it can be added that the outermost damaged surface layer, caused by previous machining processes before polishing, can be eliminated by the EP method by creating a new thickness controllable oxide film layer.

The main parameters of the EP process are electrolyte and its concentration, gap distance, current intensity, and feed rate. These parameters should be well considered to achieve an efficient process. The EP machines have a rectifier to supply direct current in which the voltage is determined by the amperes needed to electropolish the part. Generally, supplying 600–3,000 amperes requires an 18-V DC output, and 3,500–10,000 requires a 24-V rectifier. The optimum running voltage is 9–13 V for stainless steels [3]. Generally, commercial electropolishing is being done at current densities up to about 1·55 A cm^{-2} [1]. The main purpose of electropolishing is to obtain the best surface quality primarily with a suitable material removal rate.

Originally, the proposal of EP as an industrial surface finishing process was performed by Jacquet in 1930 [4]. Reliable mathematical modeling and optimizing of the electropolishing process is complicated due to existence of uncertainties related to different phenomena happen in the process. So, in the researches several optimizations have been conducted based on the experimental works and validated simulation studies for increasing the effectiveness of the process by achieving proper results of MRR and surface roughness.

Hu *et al* [5] experimentally developed a mathematical model for the surface roughness in electrochemical polishing of 304SS. Based on their work, the main factor is EP time which promotes surface roughness. The glycerol content and current density are the marginal effective parameters in their study. Men *et al* [6] investigated the electropolishing process of this material concerning the environmentally friendly electrolytes and declared the optimum processing parameters. Chen *et al* [7] simulated the driving mechanism of morphology revealed in the electropolishing process of stainless steel 304. Moayed *et al* [8] studied pitting corrosion of 304 SS electropolished in phosphoric acid and observed that the process decreases the passive current density and pitting potential.

Nunez *et al* [9] assessed the industrial electrolytes in electrochemical polishing of 316L in terms of surface roughness considering process parameters' current density, temperature, and time. Wüthrich *et al* [10] investigated the electropolishing of 316 tubings with a focus on the effect of parameters gap, tube length, and diameter on the surface roughness and claimed that voltage and duration have a more significant effect on the surface roughness and brightness. Ilman *et al* [11] studied the effect of electropolishing parameters on 316 SS to achieve the best surface roughness reduction for coronary stent application. The surface quality was investigated as an output response and working voltage, electrolyte temperature, and electropolishing time was selected as input variables. They recommended an optimized parameter to obtain 16.8% surface roughness reduction. Wei Han *et al* [12] studied electropolishing of 316L SS in a neutral salt solution of sodium chloride (NaCl) as the electrolyte without any acidic media as the commonly used electrolyte in 2020. They compared the effect of NaCl-based electrolytes with the common acidic-based electrolyte in the EP process. The reported results from experiments showed that the NaCl-based electrolyte can be a suitable alternative for the electropolishing of 316L stainless steel to reach comparable output responses with the conventional-based electrolyte.

Nakar *et al* [13] experimentally worked on surface texture and quality in electropolishing of AISI 321 tubes seeing grinding preprocess. Brent *et al* [14] focused on electropolishing capability for smoothing AM parts. They optimized the process using the Taguchi method and reported optimal parameters. In 2020 Fang and Han [15] proposed a two-step method for improving the electropolishing process employing different electrolyte

Table 1. Designed levels of input and output process parameters of EP.

Variable	Symbol	Unit	−2	−1	0	1	2
Temperature	T	[°C]	38	44	50	56	62
Current intensity	I	[A]	960	1420	1880	2340	2800
Primary Gap	PG	[mm]	0.22	0.24	0.26	0.28	0.30

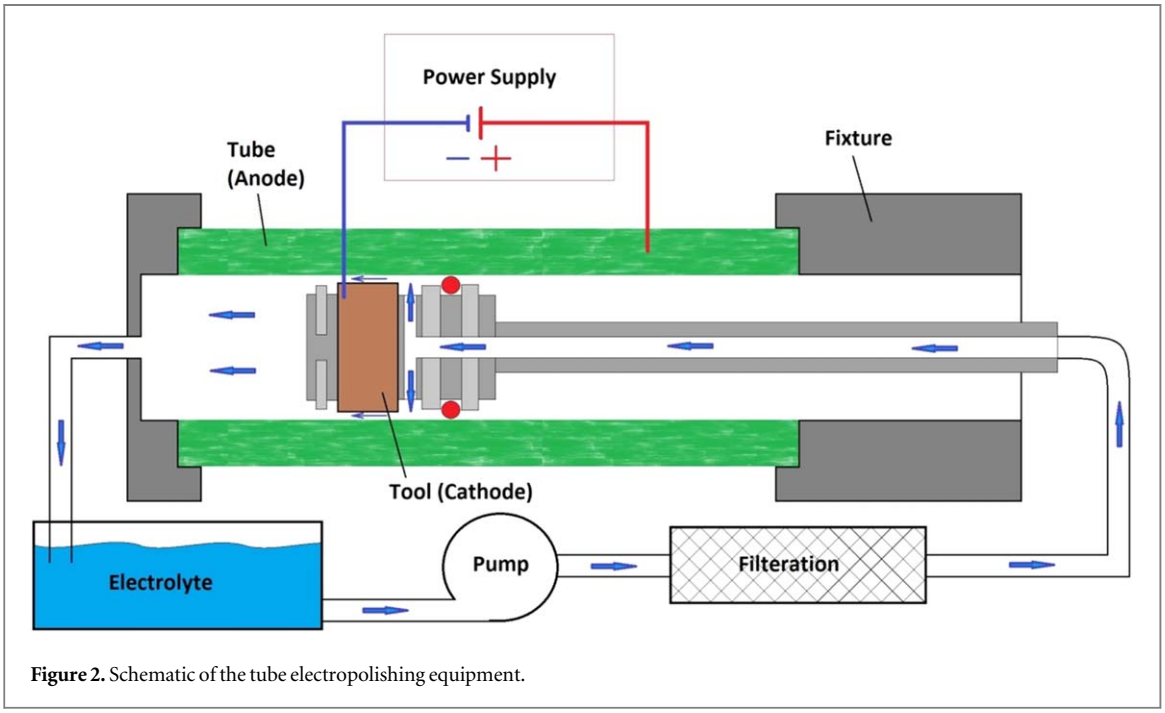

Figure 2. Schematic of the tube electropolishing equipment.

concentrations and showed that the material removal rate and surface roughness enhances consequently compared with the one-step method. In 2019 Lochynski *et al* [16] worked on the industrialization of electropolishing of stainless steel for selecting adequate parameters to achieve the greatest surface roughness results considering financial and environmental issues.

In 2020 Widlak *et al* [17] reviewed the Electrochemical Polishing of Austenitic Stainless Steels and were concerned with the process mechanism, process parameters, and process results. They presented the effects of current density, time, and the electrolyte on surface roughness, corrosion resistance, and microhardness.

In this study, the electropolishing of AISI 4340 low alloy steel in an eco-friendly NaCl-based electrolyte, not containing any acid comparing with commonly used acidic media, was performed. This process is actually a combination of a standard EP and electrochemical machining. Since fewer studies have been reported on MRR as a response to the EP process from a numerical perspective, so the main purpose of this study was to propose a simulation model for the MRR as a function of process parameters. Using this model, the process can be optimized to maximize the MRR by obtaining the appropriate surface quality without performing costly experimental tests. In addition, another aim of this study is to determine the main variables of the EP process to provide a mathematical model for MRR and surface roughness factors against input variables to control the process. In the RSM statistical approach, the proposed significant EP variables of AISI 4340 were picked out. Finally, from the results, an electropolishing model is established to illustrate the optimized parameters of AISI 4340 in the EP using Derringer's desirability technique.

2. Design of experiments and methodology

2.1. Response surface methodology (RSM)

Design of experiments (DOE) is defined as a branch of applied statistics that deals with planning, conducting, analyzing, and interpreting controlled tests to evaluate the factors that control the responses. This method helps using a minimum number of tests, in which several input variables are varied simultaneously to reach a convenient connection between them to evaluate responses. In applied statistics, response surface methodology (RSM) tracks the relationships between input variables and one or more response outputs with a mathematical basis [18]. The most demanding property of RSM is to optimize response variable which is influenced by input

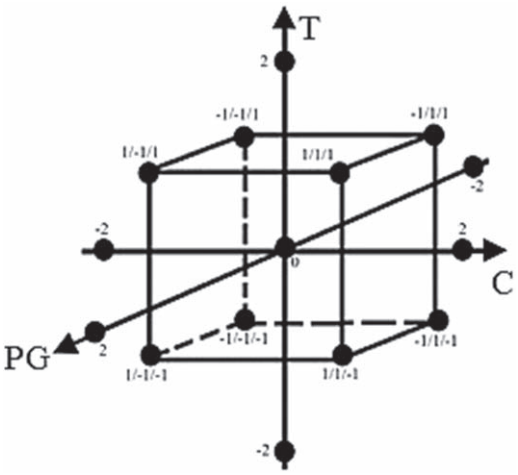

Figure 3. Cubic space with the coded levels (–2 to +2).

Figure 4. Schematic of the simulation model.

variables using an efficient minimum number of designed experiments. Due to the unknown relationship between the output response and the independent input variables, the primary step in RSM is to extract approximate relations between the responses and the used input variables [19]. In simple systems without any complexity polynomials of lower degree are employed commonly. If any curvature such as interactions is seen in the system, then polynomial of higher degree is employed necessarily. Central composite design (CCD) can be developed as a second-degree polynomial model [20]. Equation (1) shows the general form of the second-order model [21].

$$y = \beta_0 + \sum_{i=1}^{k} \beta_i x_i + \sum_{i=1}^{k} \beta_{ii} x_i^2 + \sum_i \sum_j \beta_{ij} x_i x_j + \varepsilon \quad (1)$$

β_0 is constant, β_i are linear coefficients, β_{ii} are quadratic coefficients, βij are interaction coefficients and ε is the error of each factor in the RSM model. In the regression model, for all outputs, one or more than one of these equations might be employed. It is worth mentioning that a proposed regression model will not be a precise approximation of the actual relationship between variables, but for a relatively limited area using such models is recommended commonly. In this study, the Temperature (T), Current intensity (I), and the Primary Gap (PG) were selected as independent input variables. The coded and actual values of three input parameters were shown in table 1. Figure 2 represents the mechanism of tube electropolishing equipment which is used to polish, passivate, and deburr the internal surface of the tubes. Typically, the temperature-controlled electrolyte flows inside the workpiece (anodic); and the negative pole is connected to the cathode tool. In the present study, five-level RSM with three output responses was implemented using the central composite design (CCD) strategy. This experimental design contains 15 tests; six points in the axial direction, eight as factorial points in the corners of the cube, and one in the center of the cube. Figure 3 depicts the cubic coded variables space with levels (–2 to +2) for the three response factors, according to the experimental design.

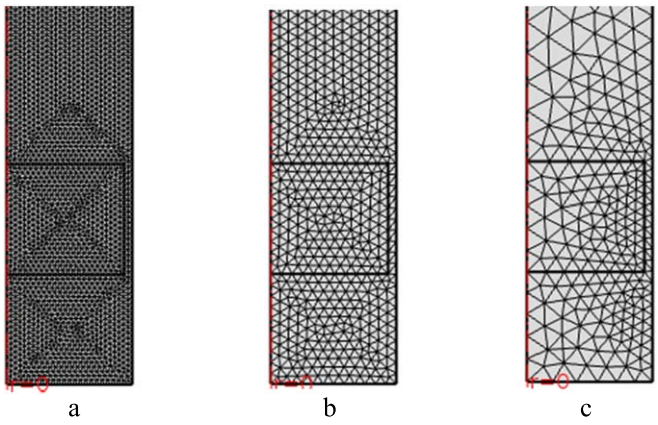

Figure 5. FEM mesh in the mesh independency analysis procedure (a) 31687 elements (b) 29006 elements (c) 927 elements.

Table 2. Mesh independency by comparing simulation with experimental criterion.

		Final gap		
Mesh elements	Initial gap	Simulation	Experimental	Error percentage (%)
31687	0.23	0.555	0.55	2.1
11446	0.23	0.556	0.55	2.6
6068	0.23	0.558	0.55	3.4
2906	0.23	0.561	0.55	4.7
1444	0.23	0.562	0.55	5.4
924	0.23	0.565	0.55	6.5

3. Finite element method simulation

In the simulations, the effect of input variables on the material removal rate of the AISI 4340 steel cylinder is investigated using COMSOL Multiphysics software. To perform the electropolishing process, a copper tool is passed through the tube according to figure 4. For this purpose, an axisymmetric geometry 2D model was created based on Matthias Hackert-Oschätzchen's [22] shape of electrolyte. The simulation model consists of two areas which the first one represents the applied copper cathodic tool with an anodic cylinder and the second area represents the geometry of the ejected electrolyte.

As mentioned above, the material removal rate was selected as output response in this study which is equal to the volume machined per unit time as equations (2) to (4).

$$MRR = \frac{Volume\ of\ WP\ before\ machining - Volume\ of\ WP\ after\ machining}{maching\ time} \tag{2}$$

$$\Delta V = \Delta A \times L \tag{3}$$

$$\Delta A = \frac{\pi}{4}(D_{2i}^2 - D_{2i}^2) \tag{4}$$

ΔV is the machined volume of the part, ΔA is the cross-section of removed material and L is the length of the electropolishing. D_{1i} and D_{2i} are the inner diameter of the cylinder before and after the polishing. The difference between the inner diameter of the workpiece and the diameter of the tool is equal to the machining gap which is somehow related to the MRR.

3.1. Meshing

The automatic mesh creator module was selected for mesh generation in the FEM model. A triangular mesh element is used for meshing. To achieve the appropriate mesh size, mesh independence analysis has been performed. Therefore, the material removal rate was simulated in different meshes and the results were compared with experimental data. According to table 2, as the number of meshes increased to 31687, the resulting error decreased to 2.1%, so this number of meshes was selected in the simulations. For calculation of the error, the difference between the simulated and experimental gap is divided by the initial value. Figure 5 shows a different number of meshes generated in the mesh independence analysis procedure.

Table 3. The conductivity of NaCl solution is measured in different temperature.

K (ohm m^{-1})	T (°C)
11.5	39
13.5	42
13.75	44
14	46
14.25	48
14.75	50
15.5	55
17.75	60

Table 4. Chemical composition of AISI 4340 low alloy steel (wt%).

	Fe	V	Ni	Cr	Mo	Mn	Si	c
X	94.42	0.080	2	2	0.3	0.7	0.15	0.3
A	55.85	50.94	58.71	52	95.94	54.94	28.09	12.011
Z	2	3	2	3	4	2	4	2
ρ (g cm^{-3})	7.89	6.1	8.9	7.19	10.2	7.43	2.33	2.26

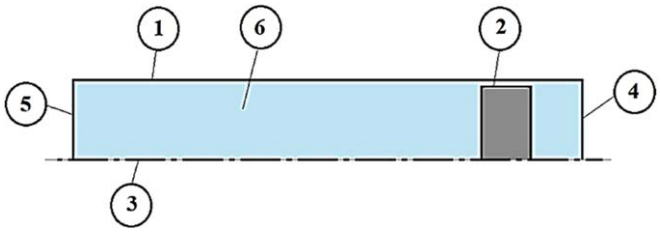

Figure 6. Simulation geometry and schematic figure of boundary conditions.

3.2. Physics

In the COMSOL multi-physics, a fully coupled model was developed for studying the material removal rate. In the model, the electric currents and deformed geometry interface were used and the material dissolution was investigated as a time-dependent study. Steel AISI 4340 (stainless steel 1.4541) was chosen from the materials library of COMSOL for the domain of the cylinder. Therefore the electrical conductivity of 4.032×10^6 S m^{-1} based on the library was assigned to this domain. The analyzes assumed that the heat generation by the viscosity and overvoltage of the electrolyte, the chemical reactions, and the heat transmitted through the electrolytes could be neglected. Because in EP, the temperature of the electrolyte is effective on anode dissolution, so the temperature-dependent properties of the electrolyte are taken into account in the simulations. Equation (5) identifies the relationship between electrolyte-specific conductivity, temperature variation, and hydrogen concentration.

$$K = K_0(1 + \alpha\Delta T)(1 - C_H)^{3/2} \tag{5}$$

where K is specific electrolyte conductivity, K_0 is specific electrolyte conductivity at the inlet to machining area, α represents the temperature coefficient of the electrolyte conductivity, C_H is hydrogen volumetric concentration; It has been assumed that the influence of dissolution products concentration on the electrolyte conductivity can be neglected.

As mentioned before, NaCl solution has been used as an electrolyte in this work. To import a linear equation for specific conductivity of electrolyte in COMSOL Multiphysics, the conductivity of the solution was measured at 8 different temperatures with a conductivity meter. The results are reported in table 3 and the equation (6) concluded.

$$K = 0.25T + 2.375 \tag{6}$$

In order to specify properties of AISI 4340 low alloy steel such as density and molar mass in COMSOL Multiphysics, we need the weight percentage of each element which is shown in table 4.

Figure 7. Electropolishing setup.

Table 5. Boundary conditions.

	Boundary	Definition
Boundary	1	Workpiece properties
	2	Polishing tool properties
	3	Axis of symmetry
	4,5	No deformation (continuity)
Domain	6	Specific conductivity of the electrolyte
	6	Potential insulation of the electrolyte

Figure 8. Conductivity meter.

The density of the alloy is calculated using equation (7).

$$\rho_a = \frac{100}{\sum_{i=1}^{n} \frac{x_i}{\rho_i}} \tag{7}$$

x_i and ρ_i are the weight percentage and density of each element and A and Z are atomic weight and atomic capacity, respectively.

3.3. Boundary conditions

The boundary conditions of the electric current interface according to figure 6 are listed in table 5.

The boundary conditions used in this model are Axis of symmetry, continuity, ground and electric potential, and electric insulation. The boundary conditions for ground and electric potential are reversed to a conventional

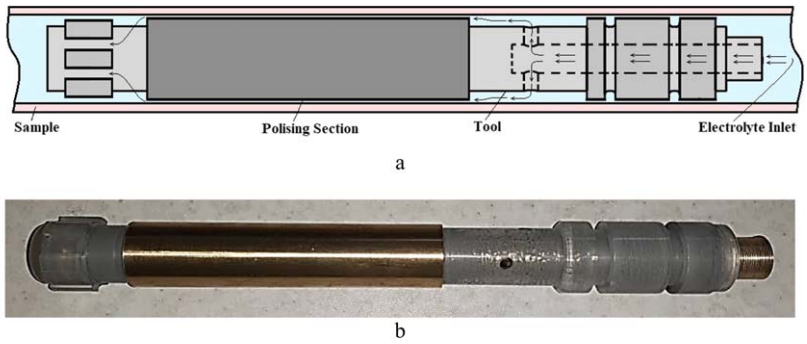

Figure 9. (a) Electrolyte path (b) polishing tool.

Table 6. Chemical composition of AISI 4340 low alloy steel (wt%).

C	Si	Ni	Mn	Cr	Mo	V	Fe
0.3	0.15	2	0.7	2	0.3	0.080	Balance

electropolishing process. The cathode surface on boundary 2 is considered as the electric ground, which means a potential of 0 V with 15.5 cm/min velocity. The surface on boundary 1 is set on the workpiece and the anodic potential of 0.27–0.55 A/mm^2 is applied. The boundaries 3, 4, 6, and 8 to 14 have been assigned to the electrical insulation.

4. Experimental work

4.1. Experimental setup

The electropolishing device, as shown in figure 7, was used to perform the experiments. This electropolishing device consists of four units. The voltage of the power supply is between 0 and 12 V and its maximum current is 3,000 A. The control system includes several electronic circuits that can measure and control the gap changes in the electropolishing process. The tool feeding unit controls the tool motion along the *Z*-axis in the machining process. The electrolyte unit includes storing, feeding, filtering, and temperature controlling the electrolyte. There is a filter that is used to prevent impure substances from entering into the machining area to ensure a clean electrolyte is in the process. To control the temperature of the electrolyte, a thermal exchanger system is employed. The electropolishing process is done in a Plexiglas's box and the workpiece is held by a particular fixture.

As mentioned above, the specific conductivity of NaCl solution in different temperatures which have been measured using a conductivity meter is shown in figure 8. CDM210 with an accuracy of ±0.2% of reading ±3 on the least significant digit was used to measure the value of conductivity and resistivity in examinations. Conductivity measurements are available in a wide range from 0.01 μS cm^{-1} to 400 mS cm^{-1} and –9.9 °C to 99.9 °C temperature.

4.2. Experiment's material

The polishing samples were AISI 4030 tubes with an internal nominal diameter of 22.5 mm (regardless of the polishing gap) and a length of 1800 mm. The chemical composition of this steel defined by quantum test and weight percentage of its alloy elements is presented in table 6. The tool was made of brass 60–40 with a diameter of 22.5 mm which its polishing section has a length of 90 mm. Figure 9(a) demonstrates a schematic diagram of the polishing tool inside the samples and the electrolyte flow path. Figure 9(b) shows the tools used in the experiments.

4.3. Output variables

4.3.1. MRR

The experimented samples were washed with distilled water and completely dried; then, the inner diameter of the cylinder was measured before and after the experiments. Since the outer diameter of the copper tool was constant, different primary gaps between anode and cathode determine the inner diameter of cylinders before polishing, whereas the final gap specifies the inner diameter of the polished cylinder. As mentioned before, the MRR was calculated using equation (2).

Table 7. Results overview.

	Input variables (Coded values)			Input variables (Actual values)			Output variables	
Sample No.	Temperature (°C)	Current (A)	Primary Gap (mm)	Temperature (°C)	Current (A)	Primary Gap (mm)	MRR (mm^3 s^{-1})	Surface roughness (Ra) (μm)
1	−1	−1	−1	44	1420	0.24	62.51	1.3
2	1	−1	−1	56	1420	0.24	50.82	1.5
3	−1	1	−1	44	2340	0.24	51.66	2.3
4	1	1	−1	56	2340	0.24	53.28	2.5
5	−1	−1	1	44	1420	0.28	50.03	1.2
6	1	−1	1	56	1420	0.28	39.98	1.1
7	−1	1	1	44	2340	0.28	41.61	1.8
8	1	1	1	56	2340	0.28	39.14	2
9	−2	0	0	38	1880	0.26	39.94	1.7
10	2	0	0	62	1880	0.26	63.35	2.2
11	0	−2	0	50	960	0.26	71.76	1.2
12	0	2	0	50	2800	0.26	61.73	2.5
13	0	0	−2	50	1880	0.22	49.99	2.3
14	0	0	2	50	1880	0.3	28.28	1.6
15	0	0	0	50	1880	0.26	60.06	2.1

Table 8. Comparing numerical and Experimental results.

				Final gap (mm)		
Gap (mm)	Current (Ampere)	Current density (A/cm^2)	Temperature (°C)	Simulation result	Experimental result	Relative error (%)
0.22	1970	47.10	42	0.545	0.56	4.4
0.22	1785	42.67	54	0.54	0.55	3
0.23	1895	45.30	39	0.555	0.54	4.8
0.23	1900	45.42	42	0.545	0.56	4.5
0.23	1890	45.18	44	0.545	0.55	1.5
0.23	1895	45.30	46	0.545	0.55	1.5
0.23	1903	45.49	51	0.56	0.55	3.1
0.24	1880	44.94	60	0.545	0.56	4.6
0.24	1635	39.09	48	0.515	0.545	9.8
0.24	1780	42.55	50	0.535	0.54	1.6
0.25	1810	43.27	45	0.55	0.55	0

4.3.2. Surface roughness (Ra)

The roughness tester device, Mahr Perthometer, was employed to measure the surface roughness (Ra) of the samples. Surface roughness [23] was measured at the beginning, middle, and the end of the part, and its average was recorded as the amount of samples' surface roughness. Before polishing, the boring process is performed on the samples so that the surface roughness (Ra) reaches approximately 2.5 μm and all samples have the same condition before the electropolishing process. Then, EP experiments were performed according to the CCD model shown in table 7 in which the measured values of responses are also demonstrated.

5. Validation of simulation model

For validating the simulation model, the obtained MRR was compared with the experimental outputs. So the final gap between anode and cathode obtained from simulation and experimental studies was compared as a representative of the MRR. The results are shown in table 8. It should be noted that in the tests, the voltage was between 6.5 to 13.5 volts. According to the results, the average difference between the experiments and simulation results was less than 3.5%.

Table 9. ANOVA analysis of the material removal rate.

Source	Sum of Squares	Degree of freedom	Mean square	F-value	P-value
Model	1906.20	4	476.55	1413.54	0.000
T	2.79	1	2.79	8.27	0.016
I	1890.95	1	1890.95	5608.93	0.000
PG	10.56	1	10.56	31.33	0.000
I^2	1.90	1	1.90	5.64	0.039
Pure Error	3.37	10	0.34		
Total	1909.57	14			
	R-Squared = 99.82%		R-Squared (Adj) = 99.75%		

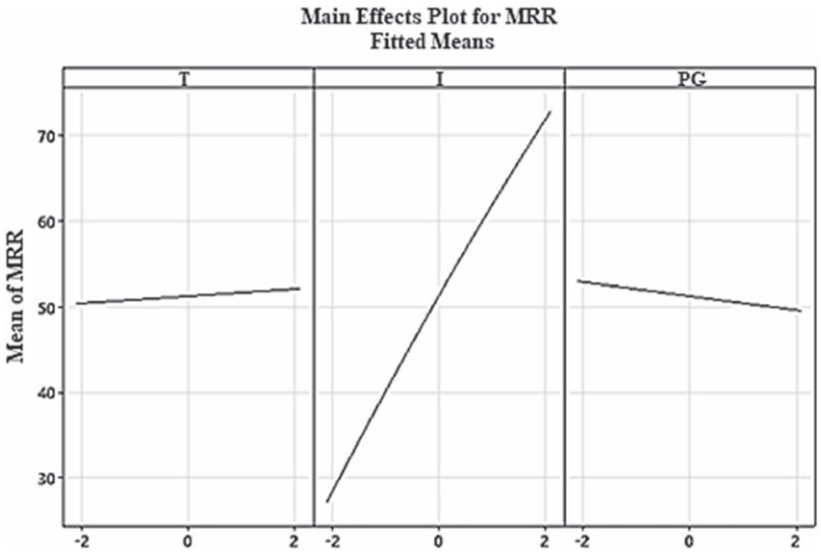

Figure 10. Main effects plot for Material Removal Rate.

6. Statistical modeling

As mentioned before, in this study the design of experiments was carried out based on the response surface methodology using Minitab software. Three levels have been considered for the input parameters electrolyte, current and primary gap, and 15 experiments have been performed, the response of which have been MRR and surface roughness as table 7. To obtain the mathematical models of responses and optimization, Analysis of variance (ANOVA) was performed; F-value and adjusted R2 parameters were used as criteria for selecting the highest polynomial order.

7. Results and discussion

ANOVA was implemented to specify significant input factors and evaluate their influences on output responses. These analyses were carried out with full quadratic polynomial functions. Statistical information about the MRR and surface roughness (Ra) as a function of variations can be extracted and analyzed by using measured values. Obviously, the obtained models will not be generalizable to other materials, but the effect of the input parameters on the outputs is probably similar for other low alloy steels.

7.1. Material removal rate

Table 9 shows details of ANOVA analysis for the MRR of polished samples. According to the table, all the main parameters have a significant effect on responses and among all quadratic terms, only the quadratic term of current (I^2) was identified as the effective one.

Equation (8) shows the regression model with coded values for the MRR in which the significant parameters have been considered.

$$MRR = 51.250 + 0.417T + 10.871I - 0.813PG - 0.288I * I \quad (8)$$

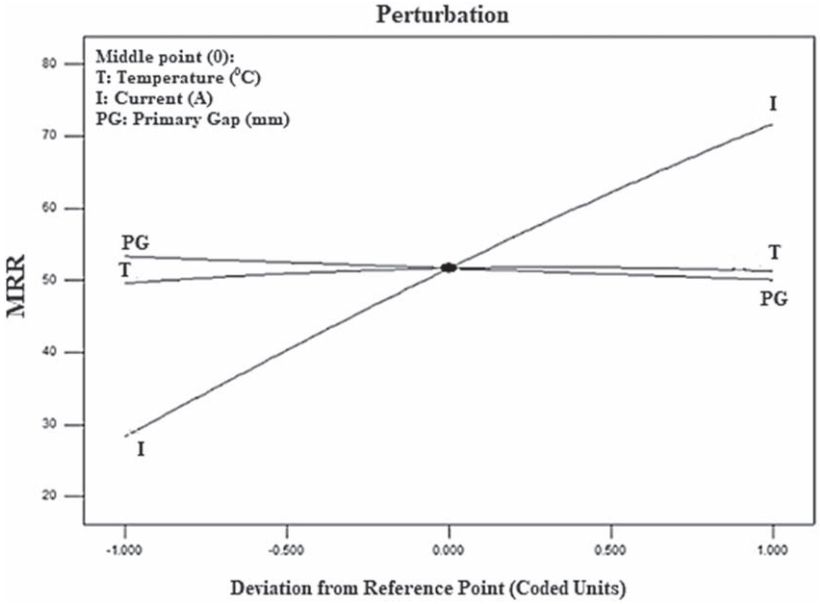

Figure 11. Perturbation plot of Material Removal Rate.

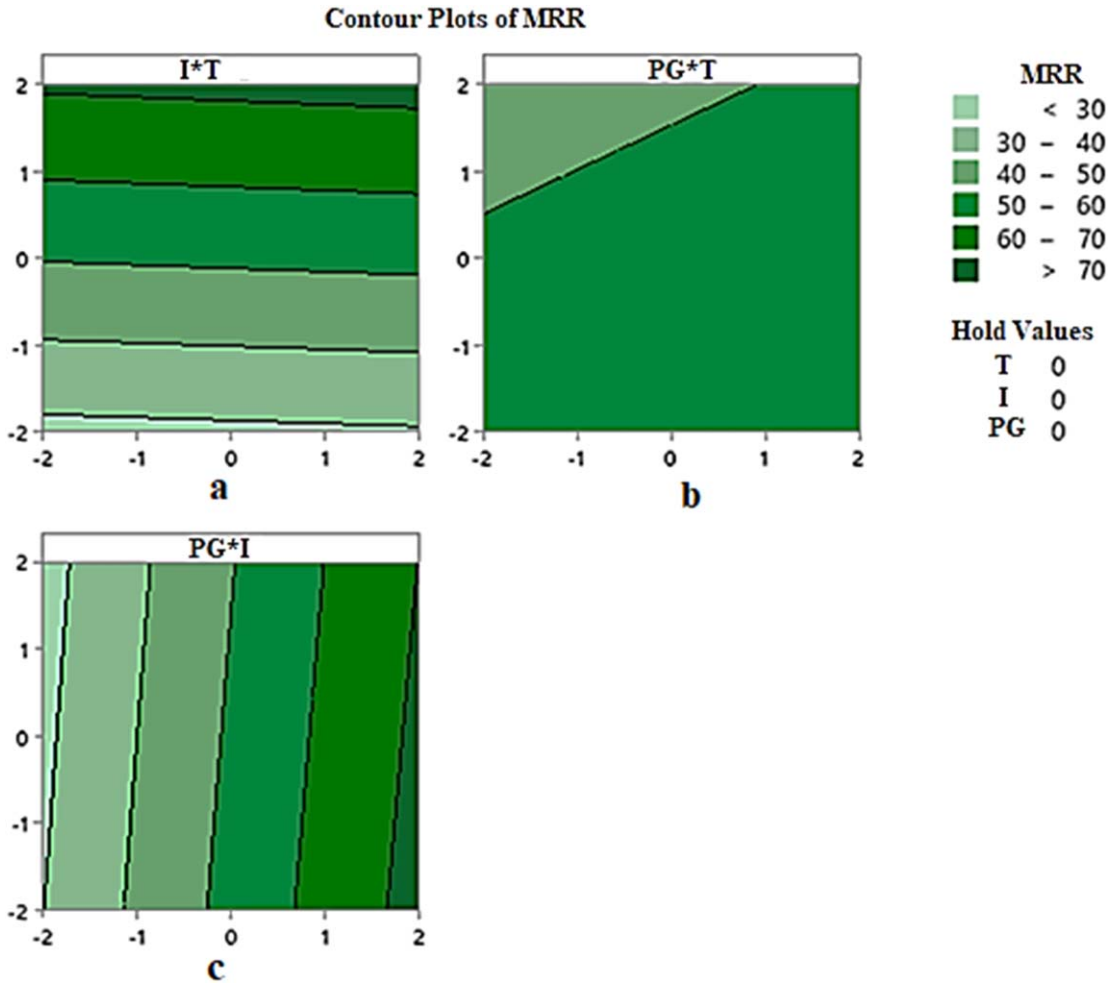

Figure 12. Contour plots of Material Removal Rate.

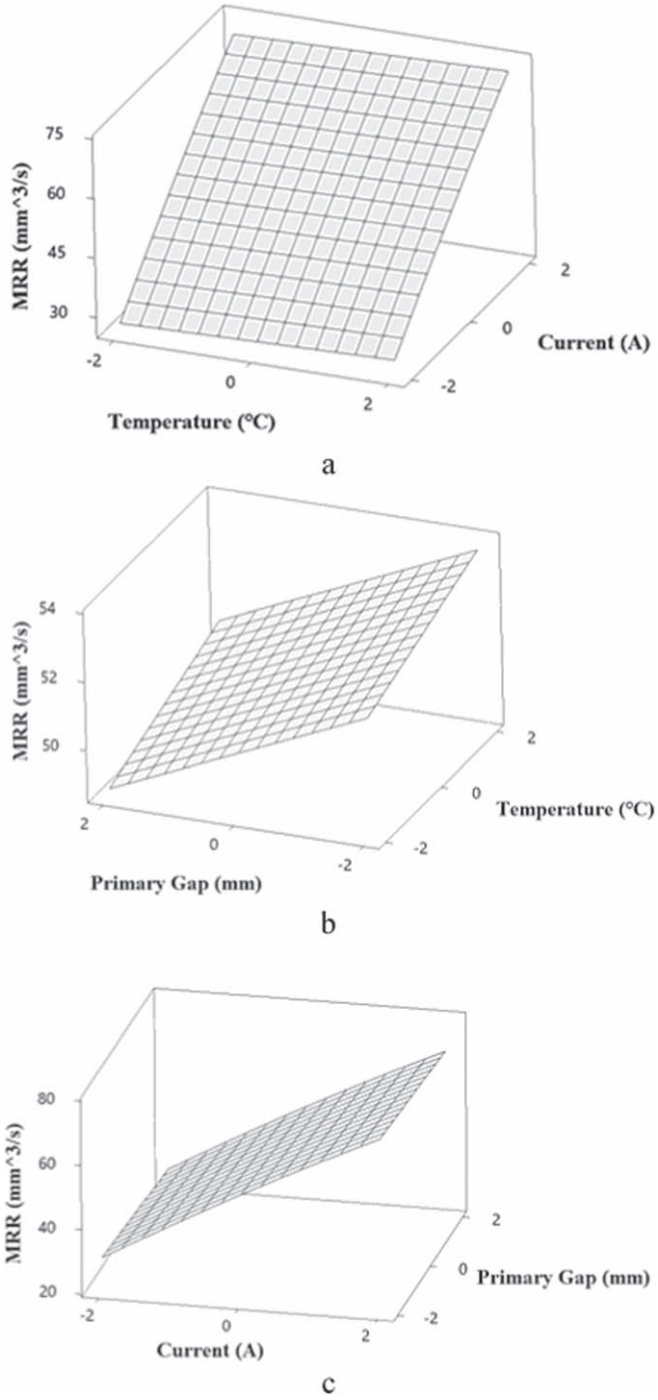

Figure 13. Response surfaces of Material Removal Rate in terms of input variables.

Figure 10 represents the main effects plot for the MRR response. The method used to assess the effect of parameters in the main effects plot is investigating the slope of lines. If the calculated line of a parameter is near horizontal, that parameter has no significant effect on the response. On the other hand, a parameter with the highest inclined line will have the most significant effect. It is obvious from the plots that factor I (current) is the most effective variable.

Figure 11 depicts the perturbation plot of material removal rate. Comparing the effect of all inputs in the central point of design space can be done with this plot. In the perturbation plot, due to plotting MRR as a response, one parameter is varying over its range whereas the other variables are kept constant. The slope of each line in the perturbation plot reveals the effectiveness of MRR to the selective parameters. From the perturbation plot, it is much obvious that the current and temperature have direct effects while the primary gap has the reverse effect on MRR.

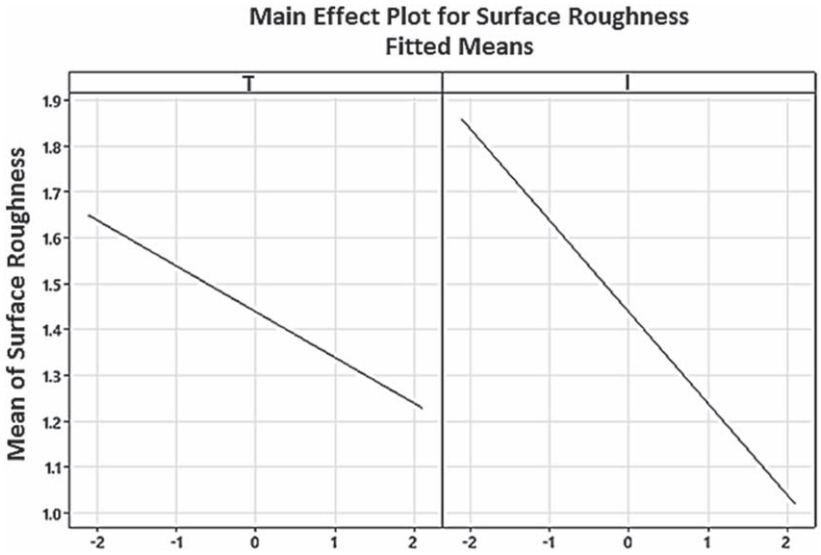

Figure 14. Main effects plot for surface roughness.

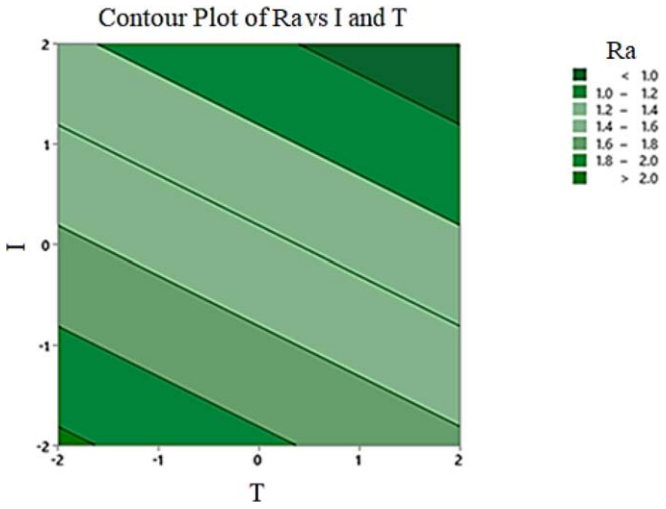

Figure 15. Contour plot of surface roughness.

Figures 12 and 13 illustrate the contour plots and response surface for MRR based on the input parameters, respectively. As can be seen in the contour plots, no interaction between input variables existed. Figures 12(a) and 13(a) show the effect of the electrolyte temperature and the current on the MRR. As the temperature increases, the electrolyte conductivity as well as the dissolution of the material increases. On the other hand, if the temperature raises enough, dissolution voltage declines, and as a result, dissolution occurs at a lower temperature and machinability improves. One of the main important reasons for the variations due to different electrolyte temperatures can be explained by the velocity of reactive ion exchange. The velocity of reactive ion exchange might be caused by kinetic and thermodynamic effects. The velocity of reactive ion exchange could be assumed to be lower at low temperatures. This influences the chemical interaction between the oxide layer and acidic solution; accordingly, the continuation of electrochemical dissolution is impaired. Furthermore, increasing the current density improves the material removal rate of the workpiece. This increase in MRR is due to the direct effect of current density on electrolysis and the separation of atoms from the workpiece surface, so that increasing the applied current density accelerates the separation of surface atoms.

Figures 12(b) and 13(b) illustrate the variation of the MRR concerning the primary gap and the temperature. MRR increases with a decrease of the inter-electrode gap. Reduction in the inter-electrode gap causes an increase in the current density in the gap with the resultant anodic dissolution. By considering the mentioned concept of the primary gap, figures 13(b) and 14(b) could be more understandable. Moreover, the influence of the temperature is mentioned above. Based on these discussions of physical phenomena, it could be concluded that

Table 10. Revised ANOVA of the surface roughness.

Source	Sum of squares	Degree of freedom	Mean square	F-value	P-value
Model	0.8	2	0.4	14.29	0.001
T	0.16	1	0.16	5.71	0.034
I	0.64	1	0.64	22.86	0.000
Pure Error	0.3360	12	0.028		
Total	1.1360	14			
	R-Squared = 70.42%		R-Squared (Adj) = 65.49%		

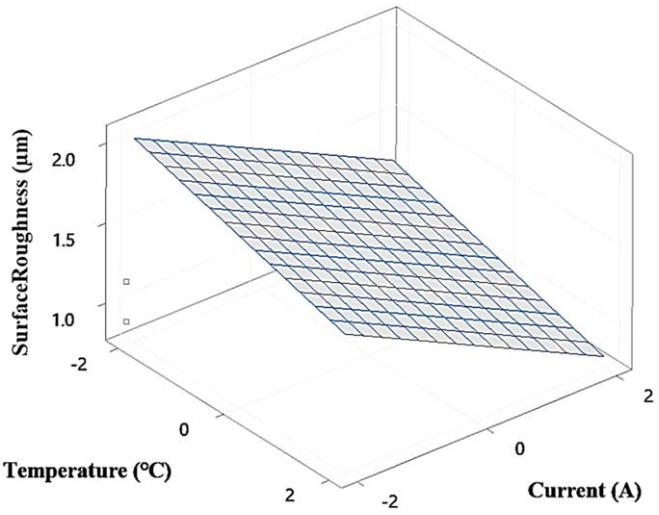

Figure 16. Response surface of Surface Roughness in terms of input variables.

Table 11. Limitations of input variables and responses.

Parameter/Response			Goal	Lower	Upper	Importance
Parameters		Temperature	in range	38	62	—
		Current	in range	960	2800	—
		Primary Gap	in range	0.22	0.3	—
Response	Criteria 1	Average Surface Roughness	Minimize	—	1.3	1
		Material Removal Rate	Maximize	60	71.76	1

reducing the primary gap of electrodes and increase the temperature will increase the MRR. According to figures 12(c) and 13(c), the MRR boosted as the current increases and the primary gap decreases. This is because the current density is severely affected by the machining gap, by reducing it, more energy is transferred to the part and the MRR increases.

7.2. Surface roughness

Table 10 shows ANOVA for the surface roughness (Ra) of polished samples. As reported, the input factors temperature and current have a significant effect on surface roughness. According to ANOVA, the quadratic and interaction terms were insignificant. Equation (9) represents the regression equation for the surface roughness considering significant parameters temperature and current.

$$SR = 1.44–0.1T–0.2I \tag{9}$$

As can be seen in figure 14 which shows the main effect plots for the surface roughness response, the parameter I (current) is the most significant parameter, obviously.

Figures 15 and 16 illustrate the 2D contour plots and 3D response surface for surface roughness based on the input parameters, respectively. As can be seen in contour plots no interactions between input variables existed. According to figure 16, by increasing the electrolyte temperature and the current, the surface roughness decreases. It has been concluded that an efficient electropolishing process can be achieved with a higher current

Table 12. Validation test and predicted result.

Solution		Optimum input parameters			Composite desirability (%)		Output responses	
		T	I	PG			Average surface roughness	Material removal rate
1	Coded value	2	2	–2	100%	Predicted	0.84	74.301
	Actual value	62	2800	0.22				

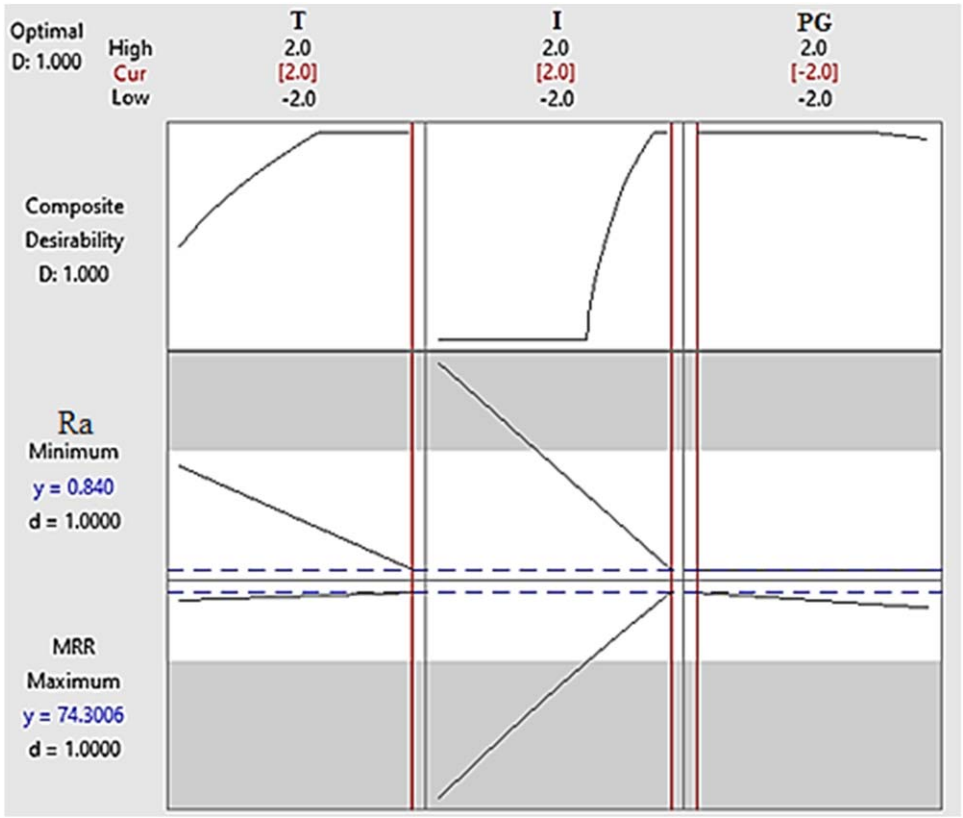

Figure 17. Derringer's desirability graph.

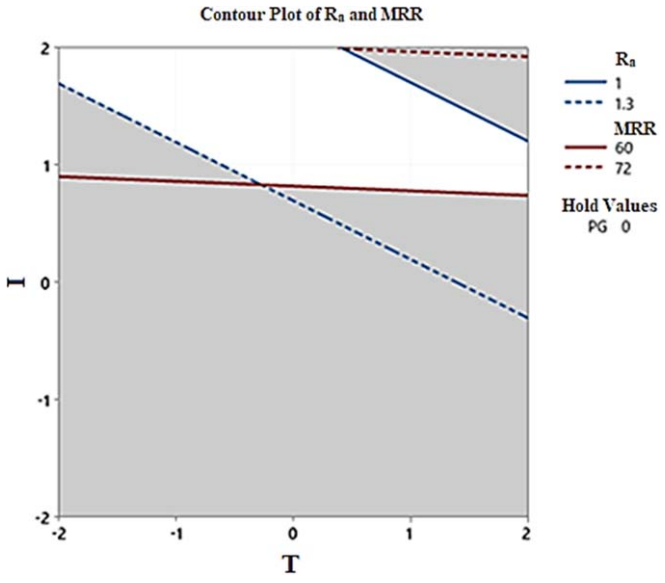

Figure 18. Overlay contour plot.

intensity. Fundamentally, the displacement rate of ions in the electrolyte is mainly affected by the electrolyte temperature.

8. Optimization

Relations between input parameters and output responses were achieved by statistically analyzing the experimental results which caused regression equations. Optimization of the EP process to reach the convenient condition with the highest desirability has been obtained by Derringer's desirability function using Minitab software [19]. Accepted limitations of the input variables and responses are obtained and shown in table 11 to optimize the Electropolishing process. The criteria of the optimization are obtained by specifying the minimum value of surface roughness and maximum value of material removal rate.

The important values of the output variables are divided equally in table 11. Optimal settings of experimental tests were carried out at the optimized predicted results due to verifying statistical analysis. Table 12 depicts the results of the validation test. Figure 17 describes Derringer's desirability with graphs.

Figure 18 illustrates an overlay plot which composed of the contour plots from each output response stacked on top of each other to create the combined plot. The created white area reveals the final optimal factor settings of experimental tests. On the other hand, the undesirable area is grayed-out. Overly plot suggests an accepted area to attain the desired condition for responses.

9. Conclusions

In this investigation, primarily a simulation model has been developed for the electropolishing process of AISI 4340 low alloy steel cylinder and validated using an experimental approach. In the following, then the effect of the electrolyte temperature, the current, and the primary gap are investigated through the Design of Experiments. According to numerical, experimental, and statistical works, the following results concluded:

- Results revealed that the electrolyte temperature and electrical current have a direct effect on the MRR while the primary gap has an inverse effect.
- The influence of parameters electrolyte temperature, current density, and the primary gap has been also investigated on surface roughness. By increasing the electrolyte temperature and the current intensity the surface roughness decreases.
- By applying a multi-response optimization, through desirability approach, the optimum settings of the EP of AISI 4340 are electrolyte temperature (T) = 62 °C, Current intensity (I) = 2800 A, primary gap (PG) = 0.22 mm.
- In the highest desired condition, the MRR of the EP process improves up to 74.301 $mm^3 s^{-1}$ and the surface roughness (Ra) up to 0.84 μm.
- Comparing the experimental and simulation results, it was found that the average error of the simulation model is 3.5%. As a result, this model shows the robustness of the present numerical model used for Electropolishing of AISI 4340.

Data availability statement

All data that support the findings of this study are included within the article (and any supplementary files).

ORCID iDs

Mohammad Meghdad Fallah https://orcid.org/0000-0002-4070-2328
Noureddine Barka https://orcid.org/0000-0003-2330-8326

References

[1] Faust C L 1964 Electrochemical machining of metals *Transactions of the IMF* **42** 355–63
[2] Yang G *et al* 2017 Electropolishing of surfaces: theory and applications *Surf. Eng.* **33** 149–66
[3] Hensel K B 2000 Electropolishing *Met. Finish.* **98** 440–8
[4] Jacquet H F A P A 1930 *French Patent* 707526

[5] Lin C-C and Hu C-C 2008 Electropolishing of 304 stainless steel: surface roughness control using experimental design strategies and a summarized electropolishing model *Electrochim. Acta* **53** 3356–63
[6] Men C L *et al* 2012 Environmental-friendly electropolishing of 304 stainless steel surface *Advanced Materials Research* **490-495** 3187–91
[7] Lee S-J, Chen Y-H and Hung J-C 2012 The investigation of surface morphology forming mechanisms in electropolishing process *Int. J. Electrochem. Sci.* **7** 12495–50612495–12506
[8] Momeni M, Esfandiari M and Moayed M H 2012 Improving pitting corrosion of 304 stainless steel by electropolishing technique *Iran. J. Mater. Sci. Eng.* **9** 34–42
[9] Núñez P *et al* 2013 Characterization of surface finish of electropolished stainless steel AISI 316L with varying electrolyte concentrations *Procedia Engineering* **63** 771–8
[10] Chaghazardi Z, Hof L and Wuthrich R 2020 Electropolishing of inside surfaces of stainless steel tubing *ECS Trans.* **97** 523
[11] Ilman K A and Herliansyah M K 2017 The effect of electropolishing parameter on 316L stainless steel surface roughness for coronary stent application *7th International Annual Engineering Seminar (InAES) (Indonesia, Aug. 1–2)* 1–6
[12] Han W and Fang F 2020 Eco-friendly NaCl-based electrolyte for electropolishing 316L stainless steel *J. Manuf. Processes* **58** 1257–69
[13] Nakar D, Harel D and Hirsch B 2018 Electropolishing effect on roughness metrics of ground stainless steel: a length scale study *Surface Topography: Metrology and Properties* **6** 015003
[14] Brent D *et al* 2016 Taguchi design of experiment for the optimization of electrochemical polishing of metal additive manufacturing components *ASME 2016 International Mechanical Engineering Congress and Exposition* V002T02A014
[15] Han W and Fang F 2020 Two-step electropolishing of 316L stainless steel in a sulfuric acid-free electrolyte *J. Mater. Process. Technol.* **279** 116558
[16] Lochyński P *et al* 2019 Electropolishing of stainless steel in laboratory and industrial scale *Metals* **9** 854
[17] Łyczkowska-Widłak E, Lochyński P and Nawrat G 2020 Electrochemical polishing of austenitic stainless steels *Materials* **13** 2557
[18] Moradi M, Arabi H and Shamsborhan M 2020 Multi-objective optimization of high power diode laser surface hardening process of AISI 410 by means of RSM and desirability approach *Optik* **202** 163619
[19] Moradi M *et al* 2021 Simulation, statistical modeling, and optimization of CO_2 laser cutting process of polycarbonate sheets *Optik* **225** 164932
[20] He Y *et al* 2018 Electrochemical machining of titanium alloy based on NaCl electrolyte solution *Int. J. Electrochem. Sci.* **13** 5736–57477
[21] Khuri A I and Mukhopadhyay S 2010 Response surface methodology *Wiley Interdiscip. Rev. Comput. Stat.* **2** 128–49
[22] Hackert-Oschätzchen M, Jahn S F and Schubert A 2011 Design of electrochemical machining processes by multiphysics simulation *COMSOL Conf.*
[23] Hanief M and Wani M 2016 Artificial neural network and regression-based models for prediction of surface roughness during turning of red brass (C23000) *Journal of Mechanical Engineering and Sciences* **10** 1835